

Explicit Symplectic Integrators for Massive Point Vortex Dynamics in Binary Mixture of Bose–Einstein Condensates

Tomoki Ohsawa*

Department of Mathematical Sciences, The University of Texas at Dallas,
800 W Campbell Rd, Richardson, TX 75080-3021, United States

(Dated: June 16, 2025)

We construct explicit integrators for massive point vortex dynamics in binary mixture of Bose–Einstein condensates proposed by Richaud *et al.* The integrators are symplectic and preserve the angular momentum of the system exactly. Our main focus is the small-mass regime in which the minor component of the binary mixture comprises a very small fraction of the total mass. The solution behaviors in this regime change significantly depending on the initial momenta: they are highly oscillatory unless the momenta satisfy certain conditions. The standard Runge–Kutta method performs very poorly in preserving the Hamiltonian showing a significant drift in the long run, especially for highly oscillatory solutions. On the other hand, our integrators nearly preserve the Hamiltonian without drifts. We also give an estimate of the error in the Hamiltonian by finding an asymptotic expansion of the modified Hamiltonian for our 2nd-order integrator.

I. MASSIVE POINT VORTEX DYNAMICS

A. Massive Point Vortices in Two-Component BEC

The main focus of this paper is to numerically solve the equations of motion for N massive point vortices in a pancake-shaped Bose–Einstein condensate (BEC) of topological charges $\{q_j = \pm 1\}_{j=1}^N$ located at $\{\mathbf{r}_j := (x_j, y_j) \in \mathbb{R}^2\}_{j=1}^N$.

We set $r_j := |\mathbf{r}_j| = (\mathbf{r}_j \cdot \mathbf{r}_j)^{1/2}$ to be the length of \mathbf{r}_j , and also use shorthands $\mathbf{r} := (\mathbf{r}_1, \dots, \mathbf{r}_N)$ and similarly for other vectors. We also set $\mathbf{e}_z := (0, 0, 1)$ and note that, for every pair of $\mathbf{a}, \mathbf{b} \in \mathbb{R}^2$, the cross product $\mathbf{a} \times \mathbf{b}$ are taken by attaching zero as the third components to both, and we see the result as a vector in \mathbb{R}^2 or \mathbb{R}^3 depending on the context.

The Lagrangian (in the non-dimensional form) for the massive N vortices in a binary mixture of BEC with components a and b is given by (see [1])

$$L(\mathbf{r}, \dot{\mathbf{r}}) := \sum_{j=1}^N \left(\frac{\varepsilon}{2} \dot{\mathbf{r}}_j^2 + q_j (\dot{\mathbf{r}}_j \times \mathbf{r}_j) \cdot \mathbf{e}_z \right) - E(\mathbf{r}), \quad (1)$$

where the parameter ε is defined as

$$\varepsilon := \frac{M_b/M_a}{N}, \quad (2)$$

where M_s with $s = a, b$ is the total mass of the components/species s ; the potential term E is given by

$$E(\mathbf{r}) := \sum_{j=1}^N \ln(1 - r_j^2) + \sum_{1 \leq j < k \leq N} q_j q_k \ln \left(\frac{1 - 2\mathbf{r}_j \cdot \mathbf{r}_k + r_j^2 r_k^2}{|\mathbf{r}_j - \mathbf{r}_k|^2} \right), \quad (3)$$

where the first term comes from a confinement to the unit disc on the plane and the second term from interactions of the N vortices. The Euler–Lagrange equation then gives

$$\varepsilon \ddot{\mathbf{r}}_j + 2q_j J \dot{\mathbf{r}}_j = -\nabla_j E(\mathbf{r}), \quad (4)$$

where $\nabla_j = \partial/\partial \mathbf{r}_j$.

The Lagrangian (1) was derived by Richaud *et al.* [1] by a variational approximation of a two-component Gross–Pitaevskii (GP) equations for a binary mixture of BECs. This was motivated by their earlier work [2] using a coupled GP equations for such a binary mixture in the immiscible regime. Specifically, solutions of the coupled GP equations show that the majority component exhibits vortices, and the atoms of the minority component are trapped inside the vortices. This results in equipping the vortices with masses, in contrast to the standard quantum vortices [3, 4] that are usually considered to be massless, and is often approximated by the Kirchhoff equations (see (14) below).

The variational approximation in [1] assumes, for the major (massless) a -species, the ansatz in the form of the trial wave function from [5] for N vortices located at $\{\mathbf{r}_j\}_{j=1}^N$, whereas it assumes, for the minor b -species, a linear combination of Gaussians from [6] centered at $\{\mathbf{r}_j\}_{j=1}^N$ as well.

We are particularly interested in the regime where $\varepsilon \ll 1$, that is, the b -species comprise a small mass compared to the a -species, but its presence is not negligible. One sees that then (4) is a singularly perturbed system.

B. Hamiltonian Formulation

Using the Lagrangian (1), the Legendre transformation is defined via the momenta $\mathbf{p} := (\mathbf{p}_1, \dots, \mathbf{p}_N)$ with

$$\mathbf{p}_j := \frac{\partial L}{\partial \dot{\mathbf{r}}_j} = \varepsilon \dot{\mathbf{r}}_j + q_j (\mathbf{r}_j \times \mathbf{e}_z) = \varepsilon \dot{\mathbf{r}}_j + q_j J \mathbf{r}_j, \quad (5)$$

* tomoki@utdallas.edu

where we set

$$J := \begin{bmatrix} 0 & 1 \\ -1 & 0 \end{bmatrix} \text{ so that } J\mathbf{a} = \mathbf{a} \times \mathbf{e}_z \quad \forall \mathbf{a} \in \mathbb{R}^2. \quad (6)$$

Hence we have $\dot{\mathbf{r}}_j = \frac{1}{\varepsilon}(\mathbf{p}_j - q_j J \mathbf{r}_j)$, and so have the Hamiltonian

$$\begin{aligned} H(\mathbf{r}, \mathbf{p}) &:= \sum_{j=1}^N \mathbf{p}_j \cdot \dot{\mathbf{r}}_j - L(\mathbf{r}, \dot{\mathbf{r}}) \\ &= \frac{1}{2\varepsilon} \sum_{j=1}^N (\mathbf{p}_j - q_j J \mathbf{r}_j)^2 + E(\mathbf{r}). \end{aligned} \quad (7)$$

Notice that the Hamiltonian is not separable, i.e., $H(\mathbf{r}, \mathbf{p}) \neq T(\mathbf{p}) + V(\mathbf{r})$ with some functions T and V . It is well known that there is no *explicit* symplectic integrator for general non-separable Hamiltonian systems [7–9].

Let us set

$$\mathbf{z}_j = \begin{bmatrix} \mathbf{r}_j \\ \mathbf{p}_j \end{bmatrix}, \quad \mathbf{z} = (\mathbf{z}_1, \dots, \mathbf{z}_N), \quad \mathbb{J}_n := \begin{bmatrix} 0 & I_n \\ -I_n & 0 \end{bmatrix},$$

where I_n is the $n \times n$ identity matrix, and consider Hamilton's equations

$$\dot{\mathbf{z}} = \mathbb{J}_{2N} \nabla H(\mathbf{z}) \iff \begin{cases} \dot{\mathbf{r}}_j = \frac{\partial H}{\partial \mathbf{p}_j}, \\ \dot{\mathbf{p}}_j = -\frac{\partial H}{\partial \mathbf{r}_j}, \end{cases} \quad (8)$$

where $j = 1, \dots, N$, or more concretely,

$$\begin{aligned} \dot{\mathbf{r}}_j &= \frac{1}{\varepsilon}(-q_j J \mathbf{r}_j + \mathbf{p}_j), \\ \dot{\mathbf{p}}_j &= \frac{1}{\varepsilon}(-\mathbf{r}_j - q_j J \mathbf{p}_j) - \nabla_j E(\mathbf{r}), \end{aligned} \quad (9)$$

noting that $q_j = \pm 1$.

C. Symplecticity and Noether Invariant

Since each vortex is constrained to the open unit disk

$$\mathcal{D} := \{\mathbf{x} \in \mathbb{R}^2 \mid |\mathbf{x}| < 1\},$$

the phase space for the Hamiltonian system (9) is

$$P := \{\mathbf{z} = (\mathbf{r}, \mathbf{p}) \in \mathcal{D}^N \times \mathbb{R}^{2N} \mid \mathbf{p} \in \mathbb{R}^{2N}\}, \quad (10)$$

which is equipped with the standard symplectic form

$$\Omega := d\mathbf{r}_j \wedge d\mathbf{p}_j = d\mathbf{x}_j \wedge d\xi_j + d\mathbf{y}_j \wedge d\eta_j, \quad (11)$$

where d stands for the exterior derivative, $\mathbf{p}_j = (\xi_j, \eta_j)$, and the summation convention is assumed on j .

Let Φ_t be the flow of (9), i.e., for every $t \in \mathbb{R}$ for which the solution $\mathbf{z}(t) = (\mathbf{r}(t), \mathbf{p}(t))$ exists with initial point $\mathbf{z}(0) = (\mathbf{r}(0), \mathbf{p}(0))$,

$$\Phi_t(\mathbf{z}(0)) = \mathbf{z}(t).$$

Then Φ_t is symplectic, i.e.,

$$\Phi_t^* \Omega = \Omega \iff D\Phi_t(\mathbf{z})^T \mathbb{J}_{2N} D\Phi_t(\mathbf{z}) = \mathbb{J}_{2N},$$

where $D\Phi_t$ stands for the Jacobian matrix of Φ_t with respect to the variables $\mathbf{z} = (\mathbf{r}, \mathbf{p})$.

One observes that the Hamiltonian (7) possesses the (planar) rotational symmetry:

$$\begin{aligned} H(R\mathbf{r}_1, \dots, R\mathbf{r}_N, R\mathbf{p}_1, \dots, R\mathbf{p}_N) \\ = H(\mathbf{r}_1, \dots, \mathbf{r}_N, \mathbf{p}_1, \dots, \mathbf{p}_N) \quad \forall R \in \text{SO}(2). \end{aligned} \quad (12)$$

As a result, the total angular momentum

$$\ell(\mathbf{r}, \mathbf{p}) := \sum_{j=1}^N (\mathbf{r}_j \times \mathbf{p}_j) \cdot \mathbf{e}_z \quad (13)$$

gives the corresponding Noether invariant, and is conserved by (9).

D. Oscillatory Solutions and Separation of Scales

The solutions of (9) tend to be highly oscillatory when $\varepsilon \ll 1$. It was also found in our recent work [10] that the initial point $(\mathbf{r}(0), \mathbf{p}(0))$ may affect the oscillatory nature of the solution. Specifically, consider the subset

$$\mathcal{K} := \{\mathbf{z} = (\mathbf{r}, \mathbf{p}) \in P \mid \mathbf{p}_j = q_j J \mathbf{r}_j \text{ for } 1 \leq j \leq N\}.$$

Notice that the Hamiltonian $H(\mathbf{r}, \mathbf{p})$ (see (7)) of the massive dynamics restricted to \mathcal{K} gives $E(\mathbf{r})$, but then this is the Hamiltonian for the massless dynamics or the Kirchhoff equations:

$$2q_j \dot{x}_j = \frac{\partial E}{\partial y_j}, \quad 2q_j \dot{y}_j = -\frac{\partial E}{\partial x_j}, \quad (14)$$

which follows from the Euler–Lagrange equation (4) by taking the limit $\varepsilon \rightarrow 0$.

It was proved in [10] that the massive dynamics—solutions of (9)—with $(\mathbf{r}(0), \mathbf{p}(0)) \in \mathcal{K}$ stays $O(\varepsilon)$ -close to \mathcal{K} for short time. It was also observed numerically in [10] that the massive dynamics with $(\mathbf{r}(0), \mathbf{p}(0)) \notin \mathcal{K}$ exhibits fast oscillations with characteristic time of scale $O(\varepsilon)$, whereas if $(\mathbf{r}(0), \mathbf{p}(0)) \in \mathcal{K}$ then such oscillations subside and the massive dynamics behaves like the massless dynamics (14) with characteristic time of scale $O(1)$. Hence \mathcal{K} is called the *kinematic subspace* in [10] in the sense that this is a domain in the phase space P where the massive dynamics effectively loses its mass/inertia and hence the dynamics becomes more massless/kinematic.

Intuitively, the highly oscillatory behaviors come from the kinetic-energy/inertia terms in $H(\mathbf{r}, \mathbf{p})$ that are proportional to $1/\varepsilon$. These terms vanish on \mathcal{K} and hence the fast (oscillatory) dynamics becomes less prominent near \mathcal{K} ; as a result, the dynamics is dominated by the slow dynamics (14) driven by $E(\mathbf{r})$.

Such a separation of scales in ordinary differential equations (ODEs) poses a stiff problem—a class of ODEs that are challenging to solve numerically because of a disparity in the time scales of the rapid transient behaviors and the slower global behaviors [11].

E. Illustrative Example: Single Massive Vortex

In order to illustrate the characteristics of the system (9) described above, let us consider a simple example of a single massive vortex ($N = 1$) with charge $q_1 = 1$ and $\varepsilon = 0.01$. Note that, although the interaction terms in E are absent, there is still the confinement term—the first term on the right-hand side in (3)—in this system. As a result, one expects to observe fast oscillations and the separation of time scales described above.

Let us consider the initial condition

$$\mathbf{r}(0) = \begin{bmatrix} 0.5 \\ 0.3 \end{bmatrix} \quad \mathbf{p}(0) = \begin{bmatrix} 0.3 \\ -0.5 \end{bmatrix} \quad (15)$$

that satisfies $(\mathbf{r}(0), \mathbf{p}(0)) \in \mathcal{K}$, as well as the one with the same $\mathbf{r}(0)$ from above but with the second component of $\mathbf{p}(0)$ from above reversed:

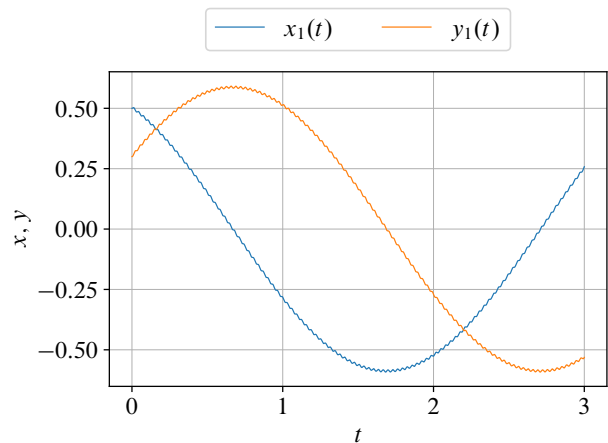
$$\mathbf{r}(0) = \begin{bmatrix} 0.5 \\ 0.3 \end{bmatrix} \quad \mathbf{p}(0) = \begin{bmatrix} 0.3 \\ 0.5 \end{bmatrix}, \quad (16)$$

for which $(\mathbf{r}(0), \mathbf{p}(0)) \notin \mathcal{K}$.

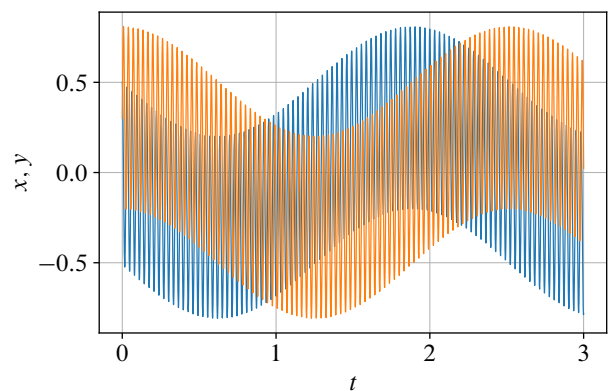
Figure 1 shows the time evolution of the (x, y) -coordinates of the single massive vortex, computed by the 4th-order symplectic method we shall construct below; see (20) and (21) below with $n = 4$. The solution with $(\mathbf{r}(0), \mathbf{p}(0)) \in \mathcal{K}$ exhibits only small fluctuations that are barely visible on the plot in panel (a), and seems to be dominated by the slow dynamics. On the other hand, the solution with $(\mathbf{r}(0), \mathbf{p}(0)) \notin \mathcal{K}$ in panel (b) shows a much more prominent combination of fast and slow dynamics.

II. SPLITTING INTEGRATORS FOR MASSIVE POINT VORTEX DYNAMICS

We would like to solve (9) numerically, with a particular focus on long-time (near-)preservation of both the Hamiltonian (7) and the angular momentum (13). As mentioned above, there is no explicit symplectic integrator for general non-separable Hamiltonian systems, although there are such integrators for specific classes of non-separable Hamiltonian systems [12–22]. There are explicit integrators for an extended Hamiltonian system defined by doubling the dimension of a general non-separable one [23, 24]. However, they are symplectic only in the extended phase space, and need to be corrected with an implicit projection to be rendered symplectic in the original phase space [25, 26].



(a) Initial condition (15) with $(\mathbf{r}(0), \mathbf{p}(0)) \in \mathcal{K}$



(b) Initial condition (16) with $(\mathbf{r}(0), \mathbf{p}(0)) \notin \mathcal{K}$

FIG. 1: Time evolution of (x, y) -coordinates of single massive vortex: $N = 1$, $q_1 = 1$, $\varepsilon = 0.01$.

A. Splitting the Hamiltonian

Our integrators are based on the following splitting of the Hamiltonian: $H(\mathbf{r}, \mathbf{p}) = \frac{1}{\varepsilon} H_A(\mathbf{r}, \mathbf{p}) + H_B(\mathbf{r}, \mathbf{p})$ with

$$H_A(\mathbf{r}, \mathbf{p}) := \frac{1}{2} \sum_{j=1}^N (\mathbf{p}_j - q_j J \mathbf{r}_j)^2, \quad (17a)$$

$$H_B(\mathbf{r}, \mathbf{p}) := E(\mathbf{r}). \quad (17b)$$

The Hamiltonian system corresponding to $\frac{1}{\varepsilon} H_A$ is then the linear system

$$\dot{\mathbf{z}} = \frac{1}{\varepsilon} \mathbb{J}_{2N} \nabla H_A(\mathbf{z}) \iff \begin{bmatrix} \dot{\mathbf{r}}_j \\ \dot{\mathbf{p}}_j \end{bmatrix} = \frac{1}{\varepsilon} \begin{bmatrix} -q_j J & I \\ -I & -q_j J \end{bmatrix} \begin{bmatrix} \mathbf{r}_j \\ \mathbf{p}_j \end{bmatrix}, \quad (18a)$$

whereas the one with H_B is

$$\dot{\mathbf{z}} = \mathbb{J}_{2N} \nabla H_B(\mathbf{z}) \iff \begin{cases} \dot{\mathbf{r}}_j = 0, \\ \dot{\mathbf{p}}_j = -\nabla_j E(\mathbf{r}). \end{cases} \quad (18b)$$

B. Exact Solutions of Split Systems

Our splitting scheme to be described below is particularly simple because both systems (18a) and (18b) are exactly solvable.

Let us first solve (18a). First notice that one can write the matrix on the right-hand side as the sum of two commuting matrices

$$\begin{bmatrix} -q_j J & I \\ -I & -q_j J \end{bmatrix} = \begin{bmatrix} -q_j J & 0 \\ 0 & -q_j J \end{bmatrix} + \begin{bmatrix} 0 & I \\ -I & 0 \end{bmatrix}.$$

Thus we have

$$\begin{aligned} & \exp\left(\frac{t}{\varepsilon} \begin{bmatrix} -q_j J & I \\ -I & -q_j J \end{bmatrix}\right) \\ &= \exp\left(\frac{t}{\varepsilon} \begin{bmatrix} -q_j J & 0 \\ 0 & -q_j J \end{bmatrix}\right) \exp\left(\frac{t}{\varepsilon} \begin{bmatrix} 0 & I \\ -I & 0 \end{bmatrix}\right) \\ &= \begin{bmatrix} R(q_j t/\varepsilon) & 0 \\ 0 & R(q_j t/\varepsilon) \end{bmatrix} \begin{bmatrix} \cos(t/\varepsilon)I & \sin(t/\varepsilon)I \\ -\sin(t/\varepsilon)I & \cos(t/\varepsilon)I \end{bmatrix} \\ &= \begin{bmatrix} \cos(t/\varepsilon) R(q_j t/\varepsilon) & \sin(t/\varepsilon) R(q_j t/\varepsilon) \\ -\sin(t/\varepsilon) R(q_j t/\varepsilon) & \cos(t/\varepsilon) R(q_j t/\varepsilon) \end{bmatrix}, \end{aligned}$$

where $R(\theta) := \begin{bmatrix} \cos \theta & -\sin \theta \\ \sin \theta & \cos \theta \end{bmatrix}$. Therefore, we may write the flow Φ_t^A of the Hamiltonian system (18a) as follows:

$$\Phi_t^A(\mathbf{r}, \mathbf{p})_j = \begin{bmatrix} \cos\left(\frac{t}{\varepsilon}\right) R\left(\frac{q_j t}{\varepsilon}\right) \mathbf{r}_j + \sin\left(\frac{t}{\varepsilon}\right) R\left(\frac{q_j t}{\varepsilon}\right) \mathbf{p}_j \\ -\sin\left(\frac{t}{\varepsilon}\right) R\left(\frac{q_j t}{\varepsilon}\right) \mathbf{r}_j + \cos\left(\frac{t}{\varepsilon}\right) R\left(\frac{q_j t}{\varepsilon}\right) \mathbf{p}_j \end{bmatrix}, \quad (19a)$$

where we wrote only the j -th component ($1 \leq j \leq N$) for brevity.

On the other hand, one easily obtains the flow Φ_t^B of the Hamiltonian system (18b) as follows:

$$\Phi_t^B(\mathbf{r}, \mathbf{p})_j = \begin{bmatrix} \mathbf{r}_j \\ \mathbf{p}_j - t \nabla_j E(\mathbf{r}) \end{bmatrix}, \quad (19b)$$

again showing only the j -th component.

Notice that the A -flow Φ_t^A exhibits oscillations with period $2\pi\varepsilon$, whereas the characteristic time scale of the B -flow Φ_t^B is determined by $\nabla_j E(\mathbf{r})$; it is $O(1)$ as long as the vortices do not get too close to each other. Therefore, our splitting can be interpreted as a splitting of the dynamics of the system (9) into the fast oscillatory dynamics of the A -flow and the slow dynamics of the B -flow.

C. Symplectic Integrators

Our base method is the 2nd-order explicit integrator by the Strang splitting [27]:

$$\Phi_{\Delta t}^{(2)} := \Phi_{\Delta t/2}^A \circ \Phi_{\Delta t}^B \circ \Phi_{\Delta t/2}^A \quad (20)$$

with time step Δt . We shall refer to this method as **Split2**.

The following fundamental properties of $\Phi^{(2)}$ then follow easily from the definition:

Proposition 1. *The 2nd-order integrator $\Phi^{(2)}$ defined in (20) is symplectic and preserves the total angular momentum ℓ (see (13)) exactly.*

Proof. The symplecticity is clear because both Φ^A and Φ^B from (19a) and (19b) define Hamiltonian flows with Hamiltonians H^A and H^B from (17a) and (17b), respectively. We also see that $\Phi^{(2)}$ preserves ℓ because both Φ^A and Φ^B preserve ℓ : Notice that both H^A and H^B possess the $\text{SO}(2)$ -symmetry as in (12); hence ℓ is a Noether invariant of both Φ^A and Φ^B . \square

We can construct higher-order integrators from (20) using the symmetric Triple Jump composition (see [28–31] and [9, Example II.4.2]): Using the 2nd-order method in (20), we recursively construct an n th-order (n being even) method as follows:

$$\Phi_{\Delta t}^{(n)} := \Phi_{\gamma_3 \Delta t}^{(n-2)} \circ \Phi_{\gamma_2 \Delta t}^{(n-2)} \circ \Phi_{\gamma_1 \Delta t}^{(n-2)}, \quad (21)$$

where

$$\gamma_1 = \gamma_3 := \frac{1}{2 - 2^{1/(n-1)}}, \quad \gamma_2 := -\frac{2^{1/(n-1)}}{2 - 2^{1/(n-1)}}.$$

We shall refer to the 4th-order method $\Phi^{(4)}$ defined above as **Split4**.

However, for a 6th-order integrator, it is more efficient to use Yoshida's method:

$$\Phi_{\Delta t}^{(6),Y} := \Phi_{\gamma_7 \Delta t}^{(2)} \circ \dots \circ \Phi_{\gamma_2 \Delta t}^{(2)} \circ \Phi_{\gamma_1 \Delta t}^{(2)}, \quad (22)$$

with certain values of γ_i 's [31] (see also [9, Section V.3.2]). We shall refer to this method as **Split6Y**.

Since all these integrators are compositions of $\Phi^{(2)}$, it follows easily from Proposition 1 that the above higher-order integrators share the same properties as $\Phi^{(2)}$:

Corollary 1. *For every positive even integer n , the integrator $\Phi^{(n)}$ defined recursively by (20) and (21) are symplectic and preserve the angular momentum ℓ exactly; so does $\Phi^{(6),Y}$ from (22).*

D. Modified Hamiltonian

The above symplectic integrators do not preserve the Hamiltonian (7) exactly. However, one can use the backward error analysis to prove that the symplectic integrators do not exhibit drifts in the Hamiltonian; this in turn implies that a p -th order symplectic method maintains errors in the Hamiltonian in the order of $(\Delta t)^p$ for a long time; see, e.g., [8, Chapter 5] and [9, Chapter IX]. This is in contrast to many other non-symplectic methods that often exhibit drifts in the Hamiltonian that result in significant errors in the Hamiltonian in the long run.

The central idea of the backward error analysis of symplectic integrators for Hamiltonian systems is to show that there is a modified Hamiltonian system

$$\dot{\mathbf{z}} = \mathbb{J}_{2N} \nabla_{\mathbf{z}} \tilde{H}(\mathbf{z}; \Delta t),$$

satisfied *exactly* by, e.g., the flow $\Phi^{(2)}$ from (20), that is,

$$\frac{d}{dt}\Phi_t^{(2)}(\mathbf{z}) = \mathbb{J}_{2N} \nabla_{\mathbf{z}} \tilde{H} \left(\Phi_t^{(2)}(\mathbf{z}); \Delta t \right).$$

Note that the modified Hamiltonian \tilde{H} depends on the time step Δt .

One may prove that such \tilde{H} exists for the splitting methods like ours (see, e.g., [8, Section 5.4]). In practice, one obtains its expressions as an asymptotic series in Δt ; see, e.g., [32], [33], [34], [8, Chapter 5], [9, Chapter IX], and references therein.

For the Strang-type splitting like Split2 defined in (20), one can obtain the first few terms of the asymptotic expansion of the modified Hamiltonian \tilde{H} fairly easily as follows (see, e.g., [8, Section 5.4]): Using the Poisson bracket defined as

$$\{F, G\} := \sum_{j=1}^N \left(\frac{\partial F}{\partial \mathbf{r}_j} \cdot \frac{\partial G}{\partial \mathbf{p}_j} - \frac{\partial G}{\partial \mathbf{r}_j} \cdot \frac{\partial F}{\partial \mathbf{p}_j} \right),$$

we have

$$\begin{aligned} \tilde{H} = & \frac{1}{\varepsilon} H_A + H_B - \frac{\Delta t^2}{24} \left\{ \frac{1}{\varepsilon} H_A, \left\{ \frac{1}{\varepsilon} H_A, H_B \right\} \right\} \\ & + \frac{\Delta t^2}{12} \left\{ H_B, \left\{ H_B, \frac{1}{\varepsilon} H_A \right\} \right\} + O(\Delta t^3). \end{aligned}$$

Typically, one can then argue that the method preserves the Hamiltonian with $O(\Delta t^2)$ error for an exponentially long period of time. However, we are particularly interested in the regime with $\varepsilon \ll 1$; one then needs Δt to be $O(\varepsilon)$ or smaller to capture the highly oscillatory solution in the timescale of ε . So we observe that the $O(\Delta t^2)$ leading error terms differ in scales:

$$\begin{aligned} \tilde{H} - H = & -\frac{\Delta t^2}{24\varepsilon^2} \{H_A, \{H_A, H_B\}\} \\ & + \frac{\Delta t^2}{12\varepsilon} \{H_B, \{H_B, H_A\}\} + O(\Delta t^3). \end{aligned} \quad (23)$$

Specifically, the first term on the right-hand side is the leading term for the difference $\tilde{H} - H$ between the modified and the real Hamiltonians.

Moreover, using the expressions (17a) and (17b), one finds

$$\begin{aligned} \{H_A, \{H_A, H_B\}\} = & \sum_{j=1}^N \sum_{k=1}^N \mathbf{P}_j^T D_{jk}^2 E(\mathbf{r}) \mathbf{P}_k \\ & + 2 \sum_{j=1}^N q_j \mathbf{P}_j \cdot (\nabla_j E(\mathbf{r}) \times \mathbf{e}_z), \end{aligned}$$

where we defined $\mathbf{P}_j := \mathbf{p}_j - q_j \mathbf{J} \mathbf{r}_j$. On the other hand,

$$\{H_B, \{H_B, H_A\}\} = \|\nabla E(\mathbf{r})\|^2.$$

Notice that $\{H_A, \{H_A, H_B\}\} = 0$ when $(\mathbf{r}, \mathbf{p}) \in \mathcal{K}$ because then $\mathbf{P}_j = \mathbf{0}$. This shows that, in this case, the leading error term proportional to $\Delta t^2/\varepsilon^2$ does not contribute to the difference between \tilde{H} and H . This suggests a difference in the accuracy of preservation of H depending on whether $(\mathbf{r}(0), \mathbf{p}(0))$ is in \mathcal{K} or not.

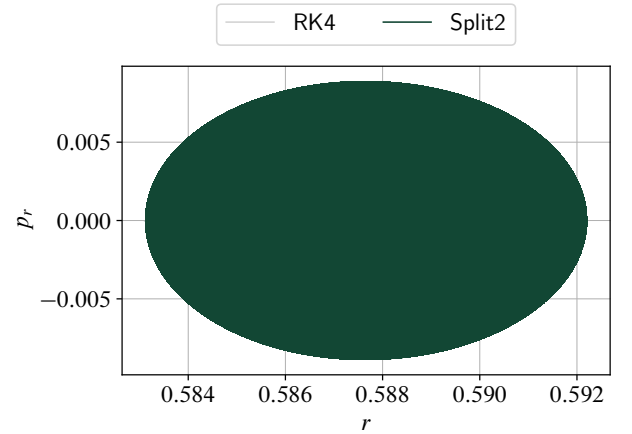
E. Testing with a Single Massive Vortex

Let us test the integrators using the single vortex example discussed in Section IE. Using the polar coordinates (r, θ) for \mathbf{r} and (p_r, p_θ) for \mathbf{p} , the Hamiltonian (7) becomes

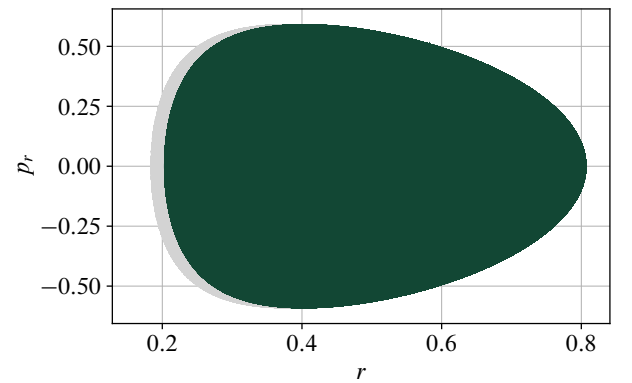
$$H = \frac{1}{2\varepsilon} \left(p_r^2 + \left(\frac{\ell}{r} + q_1 r \right)^2 \right) + \ln(1 - r^2),$$

where ℓ , the angular momentum, is an invariant of the system. Since the above expression of H depends only on (r, p_r) , the level set of H at its initial value on (r, p_r) -plane gives the trajectory $(r(t), p_r(t))$.

As in Section IE, we set $q_1 = 1$ and $\varepsilon = 0.01$, and consider the initial conditions (15) and (16), for which $(\mathbf{r}(0), \mathbf{p}(0)) \in \mathcal{K}$ and $(\mathbf{r}(0), \mathbf{p}(0)) \notin \mathcal{K}$, respectively. Then the level set of H gives a closed curve in each case.



(a) Initial condition (15) with $(\mathbf{r}(0), \mathbf{p}(0)) \in \mathcal{K}$.



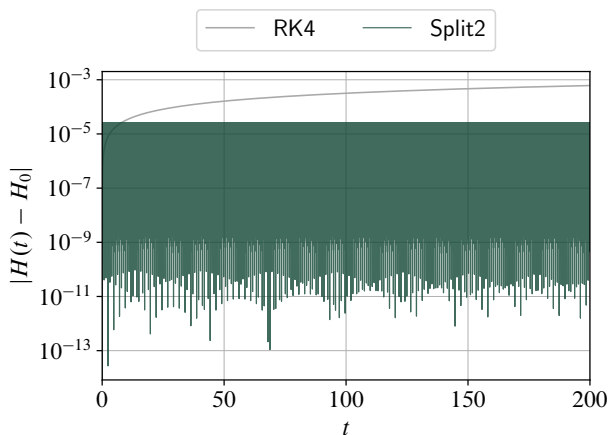
(b) Initial condition (16) with $(\mathbf{r}(0), \mathbf{p}(0)) \notin \mathcal{K}$.

FIG. 2: Phase portraits on the (r, p_r) -plane of single massive vortex dynamics for $0 \leq t \leq 200$ computed by

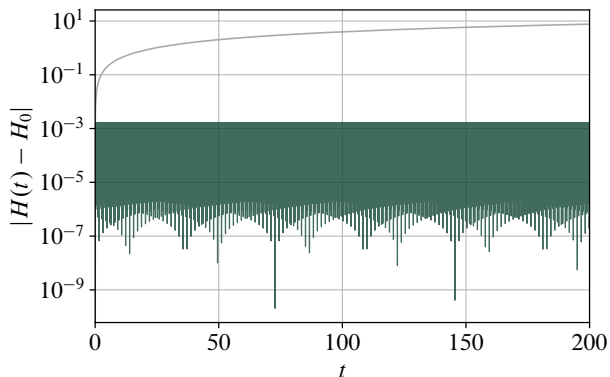
Runge–Kutta method (RK4) as well as 2nd-order splitting method (20) (Split2); $q_1 = 1$, $\varepsilon = 0.01$, and $\Delta t = 10^{-3}$.

Figure 2 shows the trajectories or the (projected) phase portraits $(\mathbf{r}(t), \mathbf{p}_r(t))$ for $0 \leq t \leq 200$ using the standard (4th-order) Runge–Kutta method (RK4) as well as our 2nd-order splitting method (20) (Split2) with the initial conditions (15) and (16), and $\Delta t = 10^{-3}$. One observes that the RK4 solution significantly deviates from a closed curve, especially in the latter case with $(\mathbf{r}(0), \mathbf{p}(0)) \notin \mathcal{K}$. On the other hand, the Split2 solution exhibits much smaller deviation from a closed curve, despite being a lower-order method than RK4. Notice also the difference in scales in the two plots: The drift in the RK4 solution in the latter case is far greater than that of the former.

Figure 3 shows the time evolution of the error in the Hamiltonian $|H(t) - H_0|$ where $H_0 := H(\mathbf{r}(0), \mathbf{p}(0))$ is the initial value of Hamiltonian H .



(a) Initial condition (15) with $(\mathbf{r}(0), \mathbf{p}(0)) \in \mathcal{K}$.



(b) Initial condition (16) with $(\mathbf{r}(0), \mathbf{p}(0)) \notin \mathcal{K}$.

FIG. 3: Time evolution of errors in Hamiltonian H for the same problem from Figure 2. The errors with Split2 are in agreement with the prediction discussed in Section II D.

Recall that, in the asymptotic expansion (23) of the modified Hamiltonian H , the first term on the right-hand side that is proportional to $\Delta t^2/\varepsilon^2$ is the leading term in the error. However, if $(\mathbf{r}, \mathbf{p}) \in \mathcal{K}$ then this leading term

vanishes, making the the second term on the right-hand proportional to $\Delta t^2/\varepsilon$ the effective leading term in the error. Since $\varepsilon = 10^{-2}$ and $\Delta t = 10^{-3}$, we have $\Delta t^2/\varepsilon = 10^{-4}$ whereas $\Delta t^2/\varepsilon^2 = 10^{-2}$. Thus we expect $|H(t) - H_0|$ to be in the order of 10^{-4} when $(\mathbf{r}(0), \mathbf{p}(0)) \in \mathcal{K}$ and 10^{-2} when $(\mathbf{r}(0), \mathbf{p}(0)) \notin \mathcal{K}$. Figure 3a and Figure 3b indeed show that the maximum errors are in those scales.

III. NUMERICAL RESULTS WITH $N = 2$

A. Massive Vortex Dipole

Consider the vortex dipole case with the following parameters and initial conditions:

$$\begin{aligned} N = 2, \quad q_1 = -1, \quad q_2 = 1, \quad \varepsilon = 0.01, \\ \mathbf{r}_1(0) = \begin{bmatrix} 0.6 \\ 0.2 \end{bmatrix}, \quad \mathbf{r}_2(0) = \begin{bmatrix} -0.3 \\ -0.4 \end{bmatrix}, \\ \mathbf{p}_1(0) = q_1 J \mathbf{r}_1(0) = \begin{bmatrix} -0.2 \\ 0.6 \end{bmatrix}, \\ \mathbf{p}_2(0) = q_2 J \mathbf{r}_2(0) = \begin{bmatrix} -0.4 \\ 0.3 \end{bmatrix}. \end{aligned} \quad (24)$$

Notice that $\mathbf{p}_j(0) = q_j J \mathbf{r}_j(0)$ so that $(\mathbf{r}(0), \mathbf{p}(0)) \in \mathcal{K}$.

We also consider another set of initial conditions with the same conditions as above except

$$\begin{aligned} \mathbf{p}_1(0) = q_1 J \mathbf{r}_1(0) + \begin{bmatrix} -0.15 \\ 0.125 \end{bmatrix} = \begin{bmatrix} -0.35 \\ 0.725 \end{bmatrix}, \\ \mathbf{p}_2(0) = q_2 J \mathbf{r}_2(0) + \begin{bmatrix} 0.075 \\ 0.2 \end{bmatrix} = \begin{bmatrix} -0.325 \\ 0.5 \end{bmatrix}, \end{aligned} \quad (25)$$

which gives $(\mathbf{r}(0), \mathbf{p}(0)) \notin \mathcal{K}$.

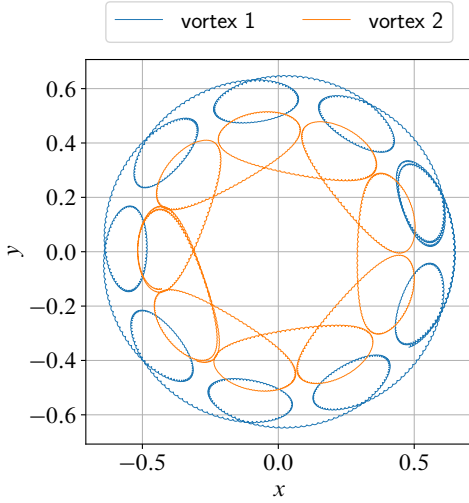
B. Comparison of Trajectories

Figure 4 shows the trajectories of both vortices for the above two sets of initial conditions, computed by Split6Y. Just as we saw in Figure 1 for the single vortex case, the trajectories have only small fluctuations in the former case with $(\mathbf{r}(0), \mathbf{p}(0)) \in \mathcal{K}$. On the other hand, for the latter case with $(\mathbf{r}(0), \mathbf{p}(0)) \notin \mathcal{K}$, the trajectories are highly oscillatory, clearly exhibiting the separation of scales as we have observed in Figure 1 for the single vortex case.

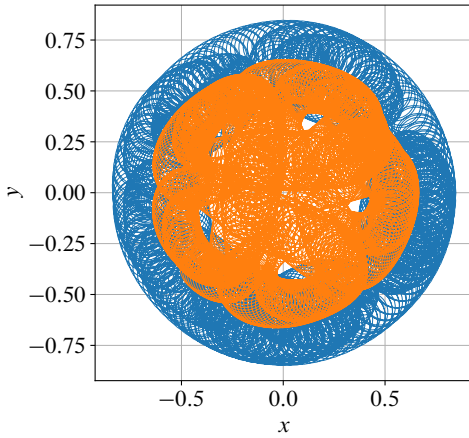
C. Comparison of Errors in Invariants

Figure 5 shows the time evolution of relative errors of two invariants—the Hamiltonian H from (7) and the angular momentum ℓ from (13)—for $0 \leq t \leq 100$ with the above initial conditions, using RK4, Split2, Split4, and Split6Y. We set the initial values of the invariants as

$$H_0 := H(\mathbf{r}(0), \mathbf{p}(0)), \quad \ell_0 := \ell(\mathbf{r}(0), \mathbf{p}(0)).$$



(a) Initial condition (24) with $(\mathbf{r}(0), \mathbf{p}(0)) \in \mathcal{K}$.

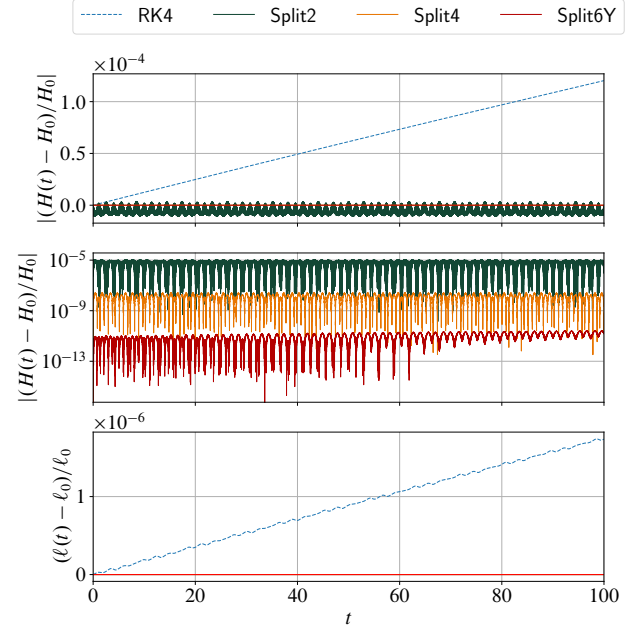


(b) Initial condition (25) with $(\mathbf{r}(0), \mathbf{p}(0)) \notin \mathcal{K}$.

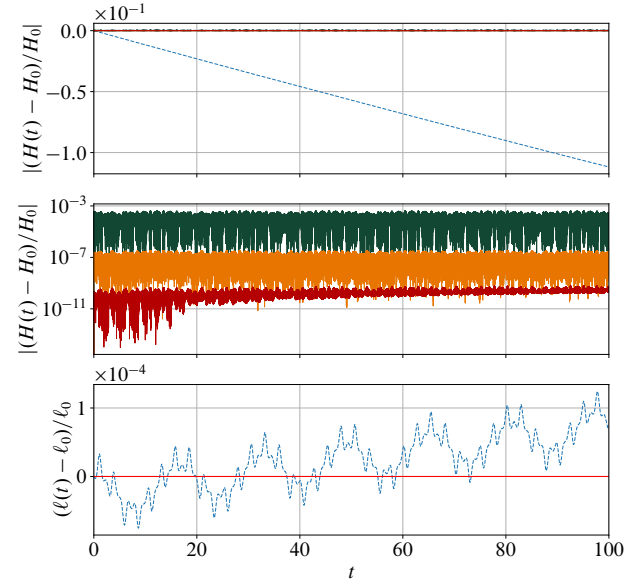
FIG. 4: Trajectories of massive vortex dipole; $N = 2$, $q_1 = -1$, $q_2 = 1$, $\varepsilon = 0.01$, and $\Delta t = 10^{-3}$; computed by Split6Y and plotted for $0 \leq t \leq 30$.

For the former case with $(\mathbf{r}(0), \mathbf{p}(0)) \in \mathcal{K}$, one observes drifts in both H and ℓ for the RK4 solution. On the other hand, the Hamiltonian for all the splitting integrators exhibit only small fluctuations near H_0 without any drifts, just as observed in Figure 2. Recall from Proposition 1 and Corollary 1 that the splitting integrators preserve ℓ exactly. One can see that the errors in ℓ for the splitting integrators are indeed negligibly small compared to that for RK4.

For the latter case with $(\mathbf{r}(0), \mathbf{p}(0)) \notin \mathcal{K}$, one sees that the drift in H for RK4 is significantly greater than the former case: the relative error grows to the order of 10^{-1} before $t = 100$ (in contrast to 10^{-4} in the former case). The relative errors in H for the splitting integrators have grown roughly by the multiplicative factor of 10^2 in comparison to the former case. This again con-



(a) Initial condition (24) with $(\mathbf{r}(0), \mathbf{p}(0)) \in \mathcal{K}$.



(b) Initial condition (25) with $(\mathbf{r}(0), \mathbf{p}(0)) \notin \mathcal{K}$.

FIG. 5: Time evolution of relative errors in Hamiltonian H and angular momentum ℓ ; $N = 2$, $q_1 = -1$, $q_2 = 1$, $\varepsilon = 0.01$, and $\Delta t = 10^{-3}$.

firms our prediction using the modified Hamiltonian that the error in H for $(\mathbf{r}(0), \mathbf{p}(0)) \notin \mathcal{K}$ is greater than that with $(\mathbf{r}(0), \mathbf{p}(0)) \in \mathcal{K}$ by the factor of $1/\varepsilon$, given that $\varepsilon = 10^{-2}$ here. However, notice that the relative errors still remain quite small compared to 10^{-1} . In particular, Split4—4th-order method just like RK4—maintains relative errors in the scale of 10^{-7} .

SUMMARY AND OUTLOOK

We have developed explicit integrators for the Hamiltonian dynamics (9) of massive point vortices that preserve the symplectic structure (11) and the angular momentum (13) exactly, as well as nearly preserve the Hamiltonian (7) without drift. Thanks to the preservation of these key invariants, the solutions exhibit excellent long-time accuracies compared to the Runge–Kutta method. In particular, in the small-mass regime $\varepsilon \ll 1$ of our interest here, the difference in accuracy is pronounced when the solutions become highly oscillatory.

Such a long-time accuracy and preservation of invariants are particularly important in numerically analyzing the stability of the massive vortices. Given a recent interest in analyzing the stability of massive point vor-

tices [35], those symplectic integrators for massive point vortex dynamics in BEC with long-time accuracy will play an important role in numerically predicting the stability of massive vortices.

It is interesting to consider an extension of our integrators to other models of massive vortex dynamics, such as those presented in [35–37], which seem to improve upon the model (9) considered here.

ACKNOWLEDGMENTS

This work was supported by NSF grant DMS-2006736. I would like to thank Andrea Richaud for introducing me to the subject of massive point vortices.

-
- [1] A. Richaud, V. Penna, R. Mayol, and M. Guilleumas, Phys. Rev. A **101**, 013630 (2020).
 - [2] A. Richaud, V. Penna, and A. L. Fetter, Phys. Rev. A **103**, 023311 (2021).
 - [3] R. Feynman, in *Progress in Low Temperature Physics*, Vol. 1, edited by C. Gorter (Elsevier, 1955) pp. 17–53.
 - [4] L. Onsager, Il Nuovo Cimento (1943-1954) **6**, 279 (1949).
 - [5] J.-k. Kim and A. L. Fetter, Phys. Rev. A **70**, 043624 (2004).
 - [6] V. M. Pérez-García, H. Michinel, J. I. Cirac, M. Lewenstein, and P. Zoller, Phys. Rev. Lett. **77**, 5320 (1996).
 - [7] J. Sanz-Serna and M. Calvo, *Numerical Hamiltonian Problems*, Dover Books on Mathematics (Dover Publications, 2018).
 - [8] B. Leimkuhler and S. Reich, *Simulating Hamiltonian dynamics*, Cambridge Monographs on Applied and Computational Mathematics, Vol. 14 (Cambridge University Press, Cambridge, 2004).
 - [9] E. Hairer, C. Lubich, and G. Wanner, *Geometric Numerical Integration: Structure-Preserving Algorithms for Ordinary Differential Equations*, 2nd ed. (Springer, Berlin, Heidelberg, 2006).
 - [10] T. Ohsawa and A. Richaud, [arXiv:2503.19222](https://arxiv.org/abs/2503.19222).
 - [11] E. Hairer, S. Nørsett, and G. Wanner, *Solving Ordinary Differential Equations II: Stiff and Differential-Algebraic Problems*, Solving Ordinary Differential Equations II: Stiff and Differential-algebraic Problems (Springer, 1993).
 - [12] J. B. Sturgeon and B. B. Laird, *The Journal of Chemical Physics*, The Journal of Chemical Physics **112**, 3474 (2000).
 - [13] S. Blanes, Physical Review E **65**, 056703 (2002).
 - [14] Y. K. Wu, E. Forest, and D. S. Robin, Physical Review E **68**, 046502 (2003).
 - [15] R. I. McLachlan and G. R. W. Quispel, BIT Numerical Mathematics **44**, 515 (2004).
 - [16] S. A. Chin, Physical Review E **80**, 037701 (2009).
 - [17] M. Tao, Journal of Computational Physics **327**, 245 (2016).
 - [18] Y. Wang, W. Sun, F. Liu, and X. Wu, The Astrophysical Journal **907**, 66 (2021).
 - [19] Y. Wang, W. Sun, F. Liu, and X. Wu, The Astrophysical Journal **909**, 22 (2021).
 - [20] Y. Wang, W. Sun, F. Liu, and X. Wu, The Astrophysical Journal Supplement Series **254**, 8 (2021).
 - [21] X. Wu, Y. Wang, W. Sun, and F. Liu, The Astrophysical Journal **914**, 63 (2021).
 - [22] X. Wu, Y. Wang, W. Sun, F.-Y. Liu, and W.-B. Han, The Astrophysical Journal **940**, 166 (2022).
 - [23] P. Pihajoki, Celestial Mechanics and Dynamical Astronomy **121**, 211 (2015).
 - [24] M. Tao, Physical Review E **94**, 043303 (2016).
 - [25] B. Jayawardana and T. Ohsawa, Mathematics of Computation **92**, 251 (2023).
 - [26] T. Ohsawa, SIAM Journal on Numerical Analysis **61**, 1293 (2023).
 - [27] G. Strang, SIAM Journal on Numerical Analysis, SIAM Journal on Numerical Analysis **5**, 506 (1968).
 - [28] M. Creutz and A. Gocksch, Phys. Rev. Lett. **63**, 9 (1989).
 - [29] E. Forest, AIP Conference Proceedings, AIP Conference Proceedings **184**, 1106 (1989).
 - [30] M. Suzuki, Physics Letters A **146**, 319 (1990).
 - [31] H. Yoshida, Physics Letters A **150**, 262 (1990).
 - [32] Y.-F. Tang, Computers & Mathematics with Applications **27**, 31 (1994).
 - [33] G. Benettin and A. Giorgilli, Journal of Statistical Physics **74**, 1117 (1994).
 - [34] S. Reich, SIAM Journal on Numerical Analysis, SIAM Journal on Numerical Analysis **36**, 1549 (1999).
 - [35] J. D’Ambroise, W. Wang, C. Ticknor, R. Carretero-González, and P. G. Kevrekidis, Phys. Rev. E **111**, 034216 (2025).
 - [36] A. Bellettini, A. Richaud, and V. Penna, The European Physical Journal Plus **138**, 676 (2023).
 - [37] A. Richaud, P. Massignan, V. Penna, and A. L. Fetter, Phys. Rev. A **106**, 063307 (2022).